THE BEHAVIOR OF TURBULENT FLOW NEAR A POROUS WALL WITH PRESSURE GRADIENT

by

Tuncer Cebeci

Report No. DAC 70014

September 1969

IRAD Technical Report

MCDONNELL DOUGLAS

24

THE BEHAVIOR OF TURBULENT FLOW NEAR A POROUS WALL WITH PRESSURE GRADIENT

by

Tuncer Cebeci

Report No. DAC 70014

September 1969

IRAD Technical Report

This report summarizes work performed at the Douglas Aircraft Company under sponsorship of the Independent Research and Development Program (IRAD) of the McDonnell Douglas Corporation.

IRAD Line Item No. D53-69-003
Fundamental Boundary Layer and Drag Studies

This report has been reviewed and is approved.

John L. Hess
J. L. Hess, Chief
Basic Research Group

11-5-69
Date

A. M. O. Smith
A.M.O. Smith,
Chief Aerodynamics Engineer
for Research

11-7-69
Date

O. R. Dunn, Director
Aerodynamics

12/10/69
Date

J. E. King
J. E. King, Director
Technology Planning

12-11-69
Date

1.0 SUMMARY

Van Driest's theory, which provides a continuous velocity and shear distribution for turbulent flow near a nonporous wall, is extended to turbulent flow near a porous wall. The new, modified theory enables the theoretical calculation of velocity profiles to be performed for a wider range of mass-transfer rates, and it gives good agreement with experimental data.

2.0 TABLE OF CONTENTS

3.0 INDEX OF FIGURES

4.0 PRINCIPAL NOTATION

c_f	local skin-friction coefficient, $\tau_w/(1/2)\rho u_e^2$
K	$(\nu_e/u_e^2)(du_e/dx)$
ℓ	mixing length
p	pressure
p^+	$-\,dp/dx\ \nu/\rho_e(u^*)^3 = K/(c_f/2)^{3/2}$
u,v	x- and y-components of velocity, respectively
u^*	friction velocity, $\sqrt{\tau_w/\rho}$
x,y	rectangular coordinates
y^+	yu^*/ν
δ	boundary-layer thickness
δ_k^*	kinematic displacement thickness, $\int_0^\infty (1 - u/u_e)dy$
θ	momentum thickness
μ	dynamic viscosity
ν	kinematic viscosity
ρ	density
τ	shear stress

Subscripts

e	boundary-layer edge
i	inner region
o	outer region
t	turbulent
w	wall

5.0 INTRODUCTION

In reference 1, Van Driest introduced a very useful modification of Prandtl's mixing length theory, which provided a continuous velocity and shear distribution for flat-plate turbulent flow near a nonporous wall. This modification also formed the basis for the theoretical calculation of the velocity profiles and has been used quite successfully by several investigators, for example by Cebeci and Smith [2], and Patankar and Spalding [3].

The purpose of this report is to show a possible method of extending Van Driest's modification to turbulent flow near a porous wall. The new modification enables the theoretical calculation of velocity profiles to be performed for a wide range of mass-transfer rates and gives good agreement with experimental data.

It is important to note that the present modification increases the capability of the Douglas boundary-layer method and allows the calculation of turbulent flows with mass transfer, which becomes quite important in boundary-layer control and drag-reduction problems, as well as in problems where it is necessary to protect surfaces exposed to high-temperature gases.

6.0 ANALYSIS

6.1 Van Driest's Analysis

Consider an infinite flat plate undergoing simple harmonic oscillation parallel to the plate in an infinite fluid. As was shown by Stokes, the amplitude of the motion diminishes from the wall, as a consequence of the factor $\exp(-y/A)$, where A is a constant depending upon the frequency of oscillation of the plate and the kinematic viscosity of the fluid. Hence, when the plate is fixed and the fluid oscillates relative to the plate, the factor $[1 - \exp(-y/A)]$ must be applied to the fluid oscillation to obtain the damping effect of the wall. By using this argument, Van Driest proposed that the mixing length ℓ in Prandtl's mixing-length theory,

$$\tau_t = \rho \ell^2 \left(\frac{\partial u}{\partial y}\right)^2 \tag{6.1}$$

should be changed to

$$\ell = \kappa y[1 - \exp(-y/A)] \tag{6.2}$$

because of the presence of the wall, since $\ell = \kappa y$ does not hold in the viscous sublayer. In dimensionless quantities Eq. (6.2) can also be written

$$\ell = \kappa y[1 - \exp(-y^+/A^+)] \tag{6.3}$$

Taking $\kappa = 0.4$ and $A^+ = 26$, Van Driest observed that calculated velocity profiles near the wall correlated very well with the experimental data. As a result, he proposed that the constant A should be

$$A = 26\nu \left(\frac{\tau_w}{\rho}\right)^{-1/2} \tag{6.4}$$

6.2 Present Analysis

The expression given by Eq. (6.4) was obtained for a flat-plate flow with no mass transfer. As it stands, it cannot be used for flows with pressure gradients. This is quite obvious, since for a flow with an adverse pressure gradient, $\tau_w \to 0$, which introduces a discontinuity in mixing-length expression and consequently in velocity profiles. It can be extended to flows with pressure gradients by the following reasoning.

Consider the momentum equation for two-dimensional incompressible turbulent flows:

$$u \frac{\partial u}{\partial x} + v \frac{\partial u}{\partial y} = - \frac{1}{\rho} \frac{dp}{dx} + \frac{1}{\rho} \frac{\partial}{\partial y} \left(\mu \frac{\partial u}{\partial y} - \rho \overline{u'v'} \right) \tag{6.5}$$

In the laminar sublayer region this equation can be written as

$$u \frac{\partial u}{\partial x} + v \frac{\partial u}{\partial y} = - \frac{1}{\rho} \frac{dp}{dx} + \frac{1}{\rho} \frac{\partial \tau}{\partial y} \tag{6.6}$$

by neglecting the Reynolds shear-stress term $-\rho\overline{u'v'}$, and by putting $\tau = \mu \, \partial u/\partial y$. If the expression (6.4) is written as

$$A = 26\nu \left(\frac{\tau}{\rho} \right)^{-1/2} \tag{6.7}$$

In other words, if τ is treated as a variable and not as a constant in the y-direction*, then for the region close to the wall, we can write Eq. (6.6) as

$$\tau = \tau_w + \frac{dp}{dx} y \tag{6.8}$$

providing that the wall is nonporous ($v_w = 0$). In that case, the expression for A should be

$$A = 26\nu \left(\frac{\tau_w}{\rho} + \frac{dp}{dx} \frac{y}{\rho} \right)^{-1/2} \tag{6.9}$$

*In reference 3, Patankar and Spalding, arguing that the local damping is more likely to be affected by the local shear stress than the damping at the extreme edge of the boundary layer, also used the local value of τ in Eq. (6.4).

which means that the pressure-gradient effect changes the damping constant A^+ to

$$A^+ = 26\left[1 + \frac{dp}{dx}\frac{y}{\rho(u^*)^2}\right]^{-1/2} \tag{6.10a}$$

Equation (6.10a) can also be written as

$$A^+ = 26\left[1 - p^+y^+\right]^{-1/2} \tag{6.10b}$$

where p^+ is an acceleration parameter defined as $p^+ = -\,dp/dx\ \nu/\rho(u^*)^3$ and y^+ is a Reynolds number defined as $y^+ = yu^*/\nu$.

In the case of a porous wall, Eq. (6.6) can be approximated as

$$\frac{d\tau}{dy} - \frac{v_w}{\nu}\tau = \frac{dp}{dx} \tag{6.11}$$

The solution of Eq. (6.11) is

$$\tau = \frac{dp}{dx}\frac{\nu}{v_w}\left[\exp\left(\frac{v_w}{\nu}y\right) - 1\right] + \tau_w \exp\left(\frac{v_w}{\nu}y\right) \tag{6.12}$$

which leads to

$$A = 26\nu\left\{\frac{dp}{dx}\frac{\nu}{\rho v_w}\left[\exp\left(\frac{v_w}{\nu}y\right) - 1\right] + (u^*)^2\exp\left(\frac{v_w}{\nu}y\right)\right\}^{-1/2} \tag{6.13}$$

As a result, the damping constant A^+ for a porous wall becomes

$$A^+ = 26\left\{\frac{dp}{dx}\frac{\nu}{\rho v_w(u^*)^2}\left[\exp\left(\frac{v_w}{\nu}y\right) - 1\right] + \exp\left(\frac{v_w}{\nu}y\right)\right\}^{-1/2} \tag{6.14a}$$

Equation (6.14a) can also be written as

$$A^+ = 26\left\{-\frac{p^+}{v_w^+}\left[\exp\left(v_w^+ y^+\right) - 1\right] + \exp\left(v_w^+ y^+\right)\right\}^{-1/2} \qquad (6.14b)$$

It should be noted that Eq. (6.14) reduces to the form given by Eq. (6.10) for pressure-gradient flows with no mass transfer and to the numerical value 26 for flat-plate flows with no mass transfer, as originally proposed by Van Driest.

It is easy to see from Eq. (6.10) that the term in brackets may be negative for highly accelerating flows. In such cases, since square root is involved, this will lead to a numerical difficulty that can easily be eliminated by taking the absolute value of the term in brackets. This was the procedure followed, for example, in reference 2. On the other hand, if we were to identify A^+ as a damping <u>constant</u> for a given streamwise location, as Van Driest did, then the above procedure is not correct. That is, A^+ in either Eq. (6.10) or (6.14) should not be a function of y^+. Consequently, it is necessary to take y^+ as a constant. Since Eq. (6.6) is valid only in the sublayer region, it will be assumed that the sublayer Reynolds number, y^+, does not deviate appreciably from the unblown flat-plate sublayer value, and it will be taken as 11.8. Equation (6.14b) then becomes

$$A^+ = 26\left\{-\frac{p^+}{v_w^+}\left[\exp\left(11.8\, v_w^+\right) - 1\right] + \exp\left(11.8\, v_w^+\right)\right\}^{-1/2} \qquad (6.14c)$$

Figure 1 shows the deviation of the damping constant from that of a flat-plate flow with no mass transfer, that is, $A^+/26$. Figure 1a shows a plot of Eq. (6.10). According to this plot, the damping constant of a pressure-gradient flow deviates considerably from that of a flat-plate flow and becomes quite large as p^+ approaches the value 0.08. This means that at large values of p^+, a condition corresponding to highly accelerating flow, the sublayer becomes larger. In this case, the skin-friction values will be lower than those obtained by $A^+ = 26$, corresponding to flat-plate flow. Figure 1b

shows a plot of Eq. (6.14c) for zero-pressure-gradient flow. It can be seen that as v_w^+ increases the damping constant decreases. In this case the region where Prandtl's unmodified mixing length applies moves closer to the wall and results in smaller sublayer thicknesses than those of flat-plate flows without mass transfer. Figure 1c is a plot of Eq. (6.14) that shows the effect of v_w^+ on the damping constant for several p^+ values. The results indicate that the damping constant increases appreciably in accelerating flows (positive p^+) and with suction increases even more, as is to be expected. Figure 1d shows the effect of p^+ on the damping constant for several v_w^+-values. As is to be expected, the damping constant increases with suction and positive p^+ and leads to larger sublayer thicknesses.

7.0 COMPARISON WITH EXPERIMENT

Needless to say, the proposed modification of Van Driest's modified mixing-length expression is empirical, and, like most expressions used in calculations of turbulent flows, it must be checked with experiment. This was done by comparing the calculated A^+-values from Eq. (6.14) with those obtained experimentally and by using the eddy-viscosity method described in reference 2. In the latter case the boundary layer is regarded as a composite layer consisting of inner and outer regions for which separate expressions for eddy viscosity are used. In other words, the solution of Eq. (6.5) is obtained by eliminating the Reynolds shear-stress term by the following eddy-viscosity formulation:

$$\epsilon = -\overline{u'v'} \Big/ \frac{\partial u}{\partial y} \tag{7.1}$$

where ϵ is given by

$$\epsilon = \begin{cases} \epsilon_i = (0.4y)^2 \left[1 - \exp\left(-\dfrac{y^+}{A^+}\right)\right]^2 \left|\dfrac{\partial u}{\partial y}\right| & 0 \le y \le y_c \qquad (7.2a) \\ \epsilon_o = 0.0168 u_e \left|\delta_k^*\right| \left[1 + 5.5\left(\dfrac{y}{\delta}\right)^6\right]^{-1} & y_c \le y \le \delta \qquad (7.2b) \end{cases}$$

and the matching point y_c between two regions is obtained from the continuity of eddy viscosity, namely, $\epsilon_i = \epsilon_o$. In Eq. (7.2a) the damping constant A^+ is given by Eq. (6.14).

Figure 2 shows the variation of damping constant A^+ with blowing parameter $\sqrt{2/c_f}\ v_w^+$. The experimental values of A^+ were obtained from the data of Simpson et al [4] and Kendall [5], and were reported in reference 6 by Bushnell and Beckwith. The figure also shows the curve faired to the experimental data used by Bushnell and Beckwith, together with the results obtained from Eq. (6.14) for zero pressure gradient. The skin-friction values for Eq. (6.14) were obtained from Simpson's data [4] for blowing and from Tennekes' data [7] for suction. The agreement between Eq. (6.14), the experimental data, and the faired curve is very good for blowing parameters up to 14. For larger blowing parameters, the calculated A^+ values deviate from the

faired curve used by Bushnell and Beckwith, but seem to agree reasonably well with experimental data except for one value.

Figures 3a, 3b, and 3c show the calculated velocity profiles obtained by the eddy-viscosity formulation given in Eq. (7.2) for blowing rates of v_w/u_e = 0.00386, 0.00784, and 0.00950, respectively, for the experimental data of Simpson et al [4]. In these calculations the damping constant A^+ as given by Eq. (6.14) was used. It is important to note that calculations could not be made with the unmodified damping constant given by Eq. (6.4). Figures 4a and 4b show a comparison of calculated and experimental skin-friction values obtained for two blowing rates, v_w/u_e = 0.00386 and 0.00784, respectively. In general, the agreement seems satisfactory, and a slight dicrepancy in skin-friction values could be due to the procedure that was followed in making comparisons. Ideally, one should start the theoretical calculations by inputting the initial velocity profile obtained from the experimental data. However, in the present comparisons, an effective length that matched the momentum thickness at the station where blowing began was determined. This procedure does not necessarily match the initial skin-friction coefficient at that station. However, as the calculations continue in the streamwise direction, the initial discrepancy in the local skin friction decreases. For example, when the comparisons were made for the blowing ratio of v_w/u_e = 0.00950, the calculated and experimental skin-friction values were 5.5×10^{-4} and 3.4×10^{-4}, respectively, at the station where the matching was made ($R_\theta = 4.3 \times 10^3$). Downstream, at sufficiently higher Reynolds number, the discrepancy became quite small. For example, at $R_\theta = 15 \times 10^3$, the experimental and calculated local skin friction values were 1×10^{-4} and 1.1×10^{-4}, respectively, and at $R_\theta = 17 \times 10^3$, they were 1×10^{-4} and 0.98×10^{-4}, respectively.

Comparisons were also made for the sucked boundary layers. The experimental data of Tennekes were used for this purpose. Figure 5 shows a comparison of calculated and experimental velocity profiles for a suction rate of v_w/u_e = -0.00312. Figures 6a and 6b show comparisons of calculated and experimental values of momentum thickness and local skin friction, respectively. In general, the agreement is quite satisfactory.

For the test cases considered in this report, the calculated results indicate that the proposed modification of Van Driest's expression is quite useful and gives good agreement with experiment. Further comparisons on the same subject, which will be reported in reference 8, also show the same good agreement and give further support to the proposed modification.

8.0 CONCLUDING REMARKS

The results show that the proposed modification of Van Driest's theory seems to be suitable for carrying the calculations right down to the wall to compute flows with pressure gradients and mass transfer. In the absence of a better empirical fit, the new formulation appears to be quite useful.

9.0 REFERENCES

1. Van Driest, E.R.: On Turbulent Flow Near a Wall. J. of Aerospace Sci., Vol. 23, No. 11 (November 1956).
2. Cebeci, T.; and Smith, A.M.O.: A Finite-Difference Solution of the Incompressible Turbulent Boundary-Layer Equations by an Eddy-Viscosity Concept. Computation of Turbulent Boundary Layers. 1968 AFOSR-IFP-Stanford Conference, Vol. 1 (1968).
3. Patankar, S.V.; and Spalding, D.B.: Heat and Mass Transfer in Boundary Layers. C.R.C. Press, Cleveland (1968).
4. Simpson, R.L.; Kays, W.M.; and Moffat, R.J.: The Turbulent Boundary Layer on a Porous Plate: An Experimental Study of the Fluid Dynamics with Injection and Suction. Report N. HMT-2. Stanford University (1967).
5. Kendall, R.M.; Rubesin, M.W.; Dahm, T.J.; and Mendenhall, M.R.: Mass, Momentum, and Heat Transfer Within a Turbulent Boundary Layer with Foreign Gas Mass Transfer at the Surface. Part 1 - Constant Fluid Properties. Rept. No. 111, Vidya, Division of Itek Corp., (Feb. 1964).
6. Bushnell, D.M.; and Beckwith, I.E.: Calculation of Nonequilibrium Hypersonic Turbulent Boundary Layers and Comparisons with Experimental Data. AIAA Preprint No. 69-684.
7. Tennekes, H.: Similarity Laws for Turbulent Boundary Layers with Suction or Injection. Report VTH-119. Technological University, Delft, (Dec. 1964).
8. Cebeci, T.; and Mosinskis, G.: Calculation of Heat and Mass Transfer in Turbulent Flows at Low Mach Numbers. Douglas Report No. DAC 70015 (1969).

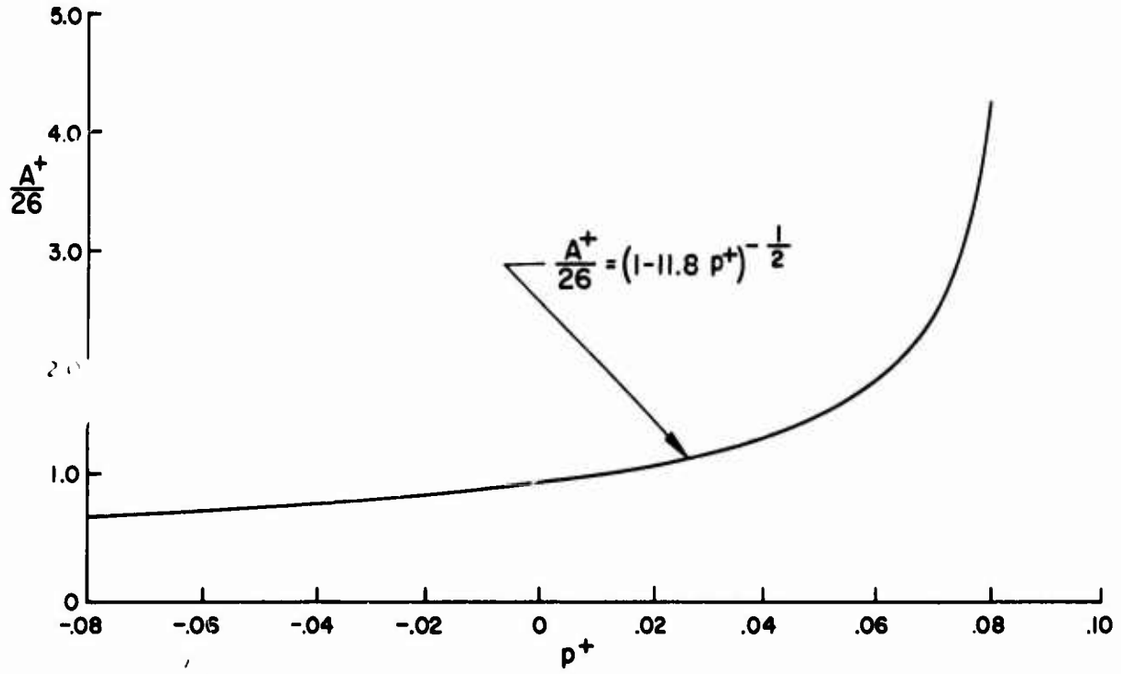

Figure 1a. Deviation of damping constant of a pressure gradient flow from that of a nonporous flat-plate flow.

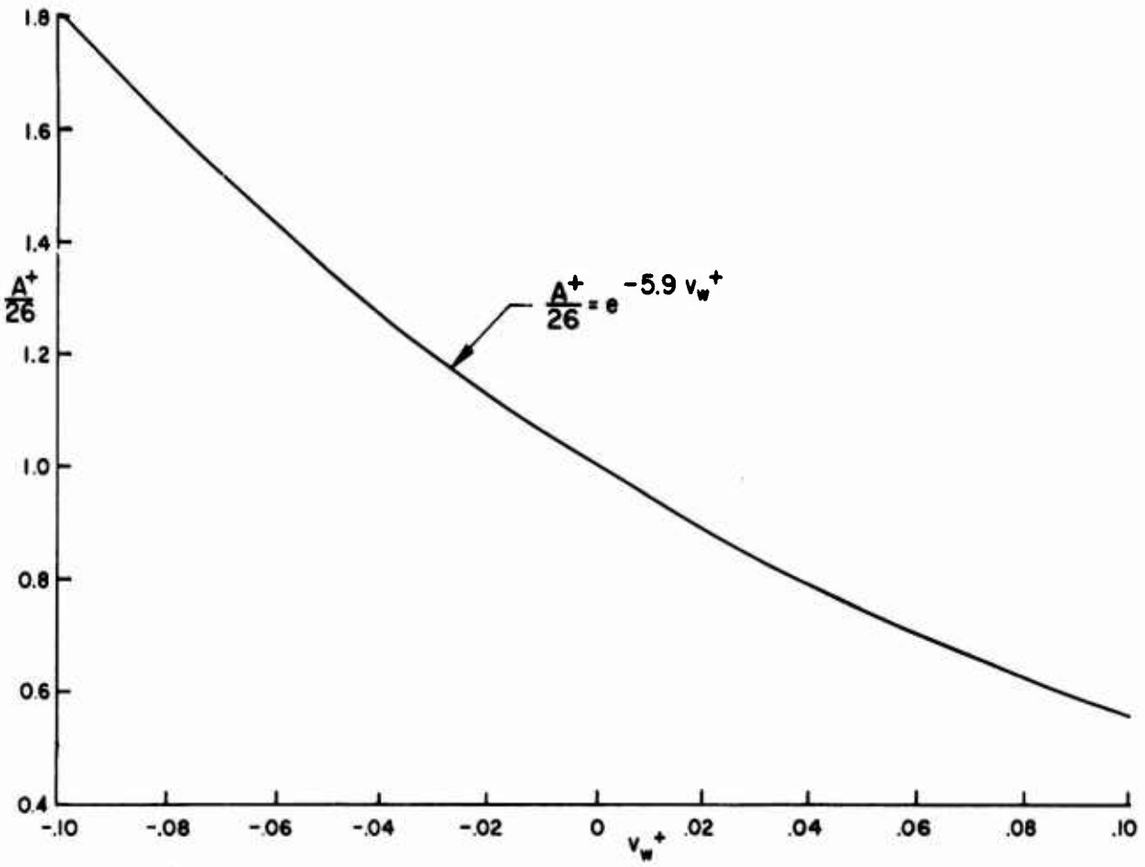

Figure 1b. Deviation of damping constant of a porous flat-plate flow from that of a nonporous flat-plate flow.

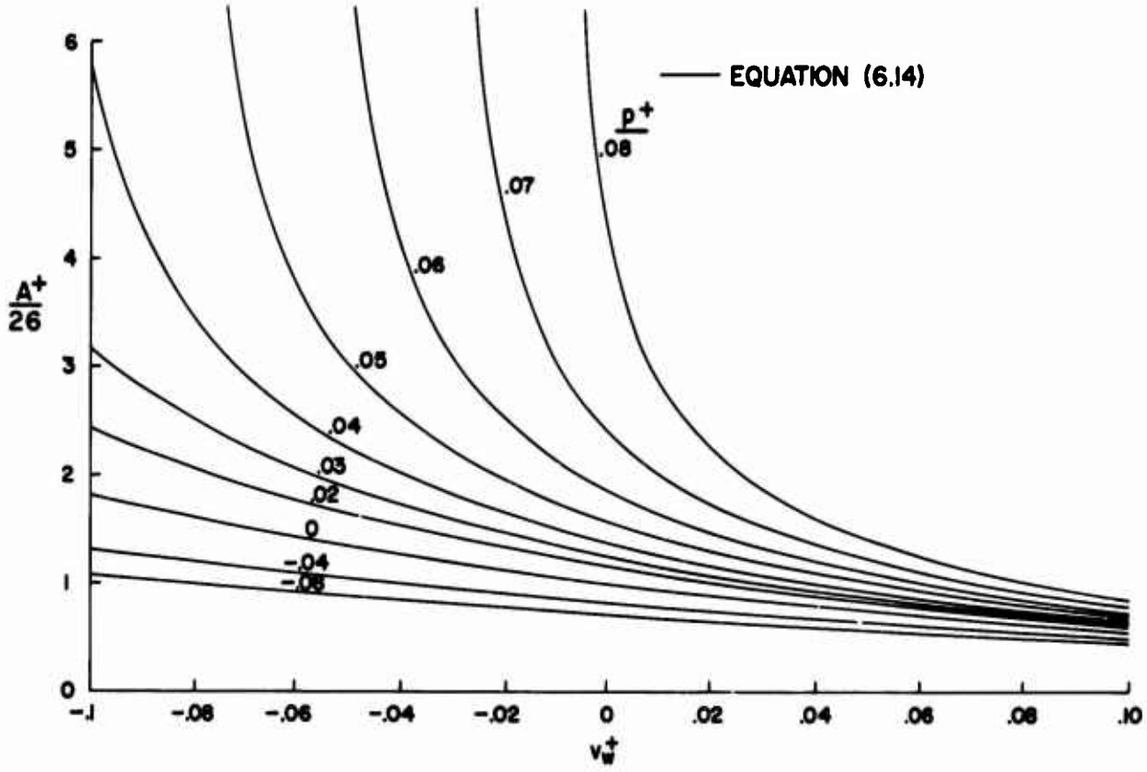

Figure 1c. Deviation of damping constant with blowing parameter v_w^+ for several p^+ values.

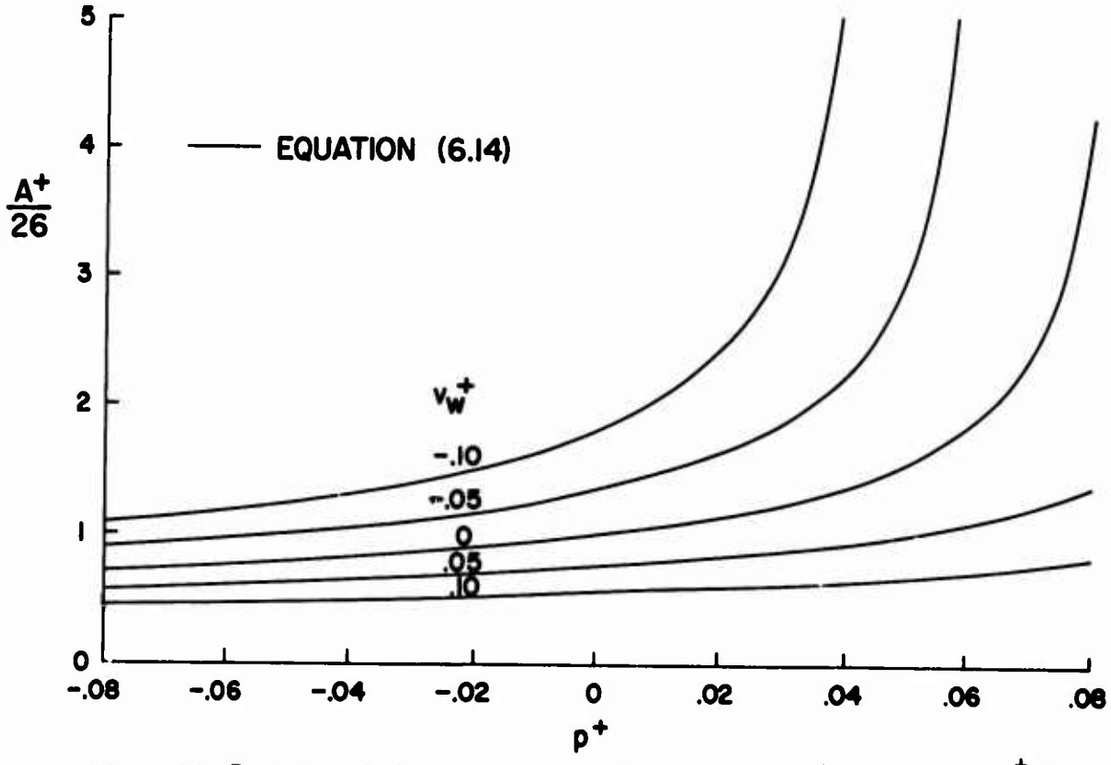

Figure 1d. Deviation of damping constant with pressure gradient parameter p^+ for several v_w^+ values.

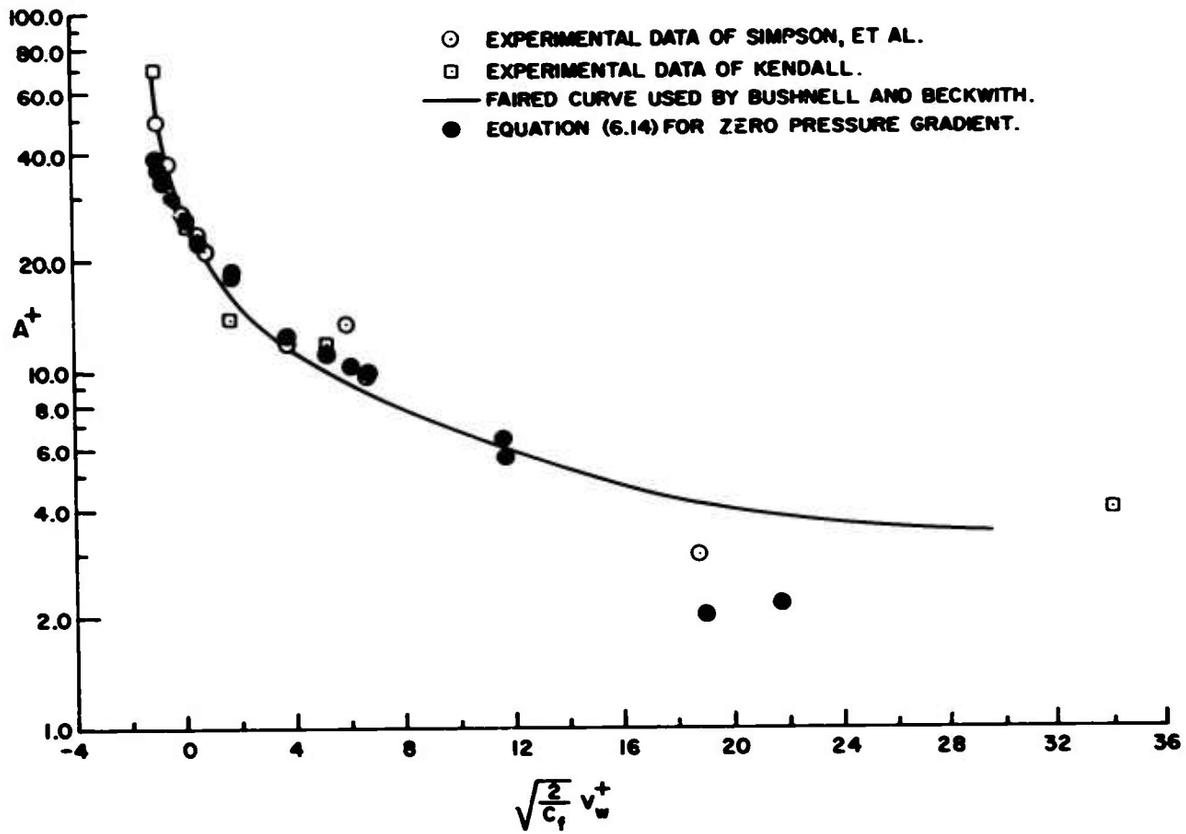

Figure 2. Comparison of calculated and experimental damping constants for a flat-plate flow with mass transfer.

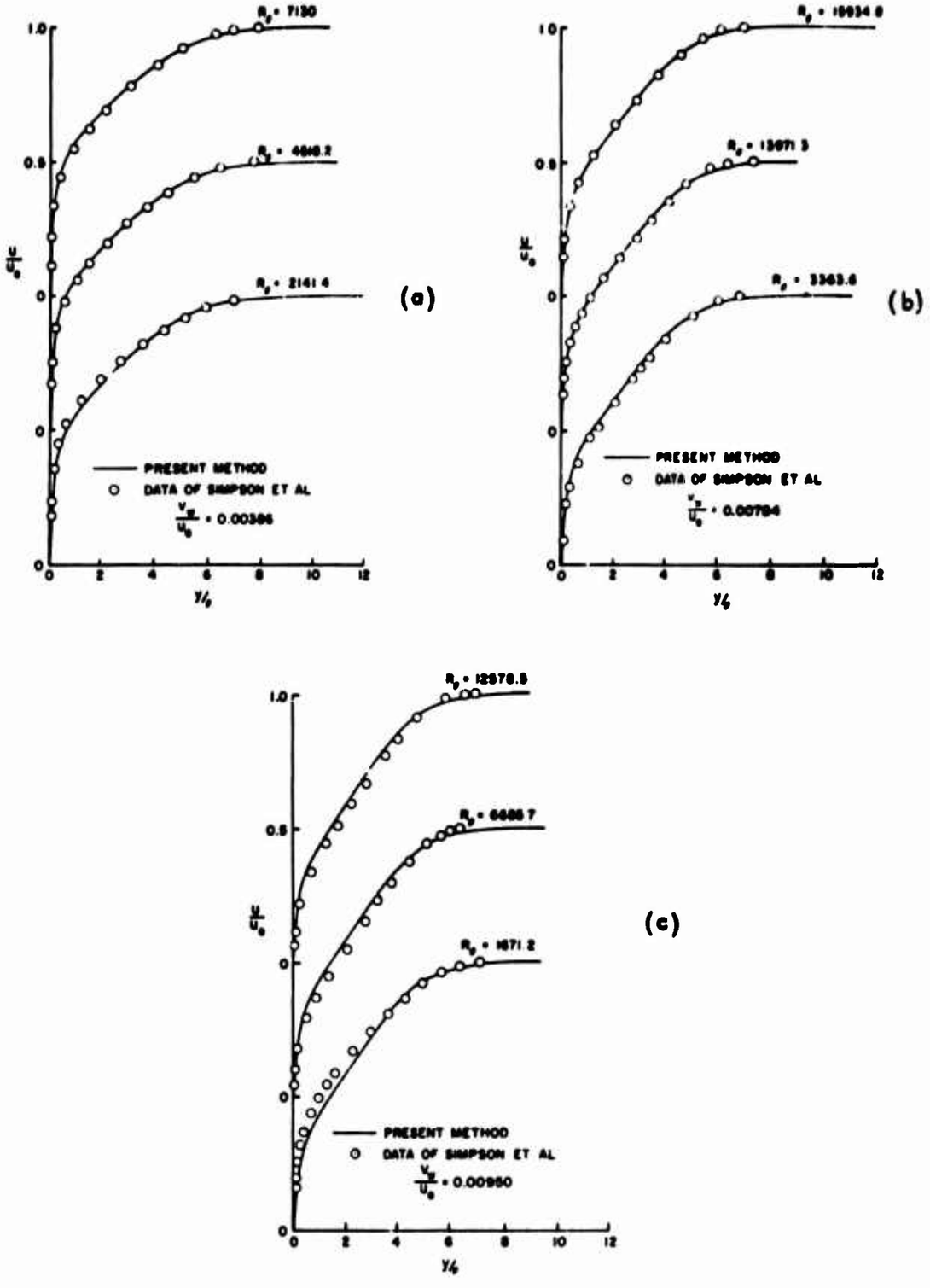

Figure 3. Comparison of calculated and experimental velocity profiles for the blown boundary layer measured by Simpson et al [4]; (a) v_w/u_e = 0.00386, (b) v_w/u_e = 0.00784, (c) v_w/u_e = 0.00950.

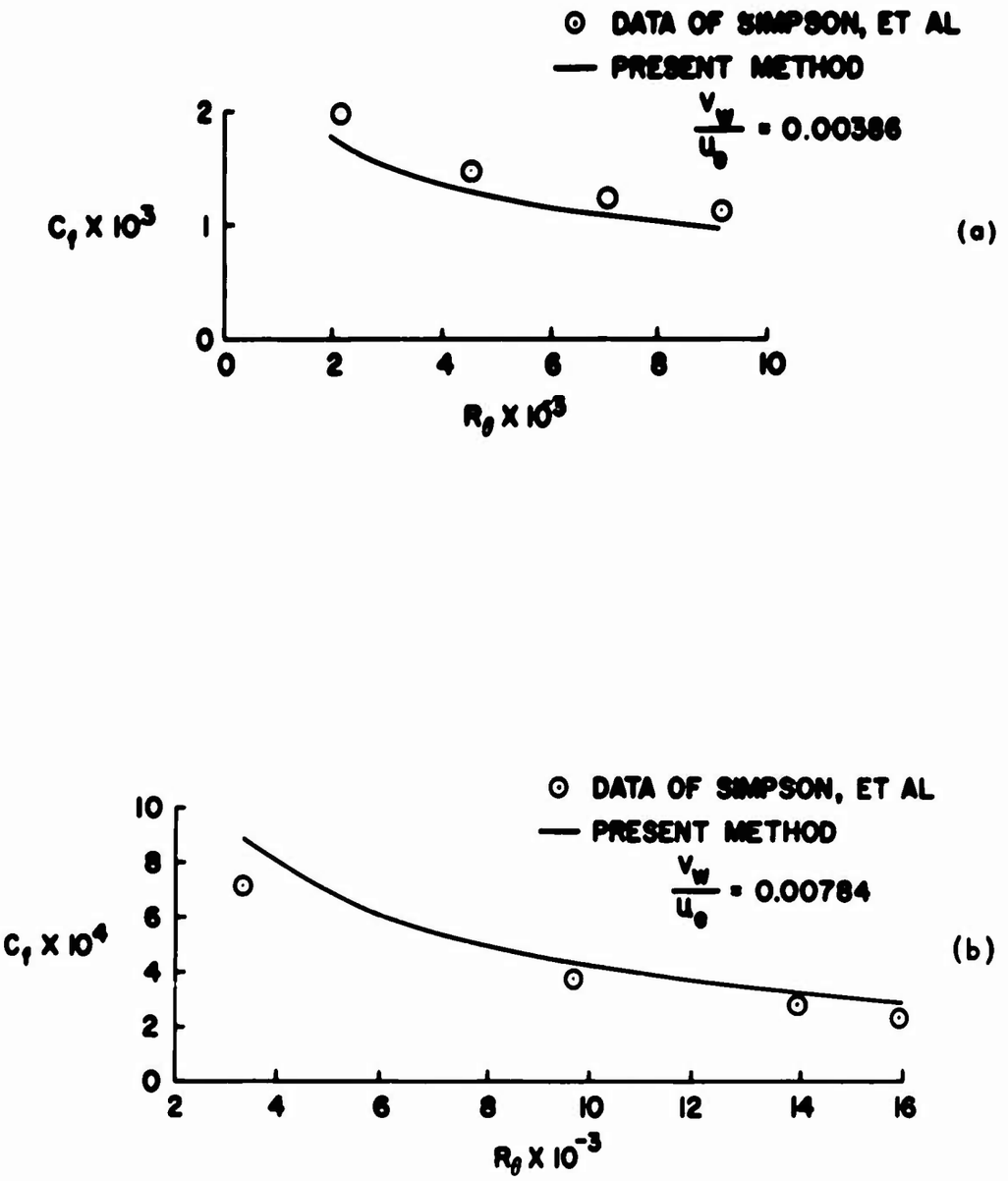

Figure 4. Comparison of calculated and experimental skin friction values for the blown boundary layer measured by Simpson et al [4]; (a) v_w/u_e = 0.00386, and (b) v_w/u_e = 0.00784.

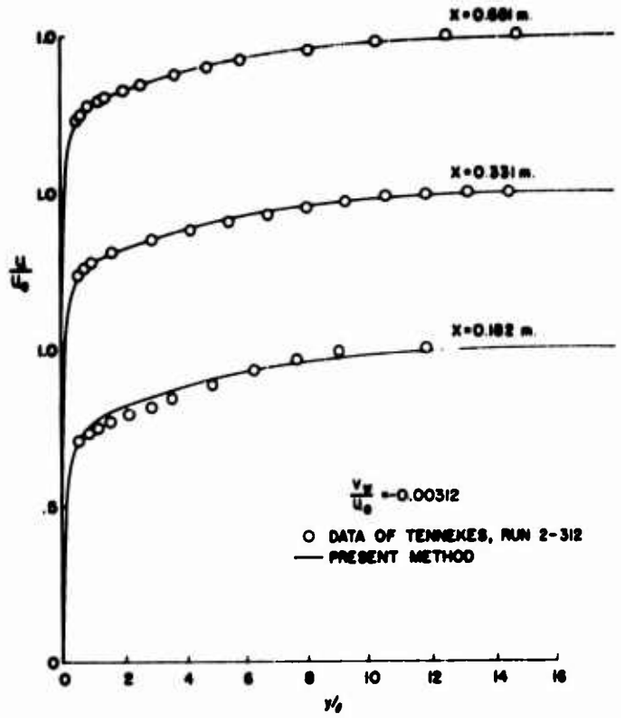

Figure 5. Comparison of calculated and experimental velocity profiles for the sucked boundary layer measured by Tennekes [7] for $v_w/u_e = -0.00312$.

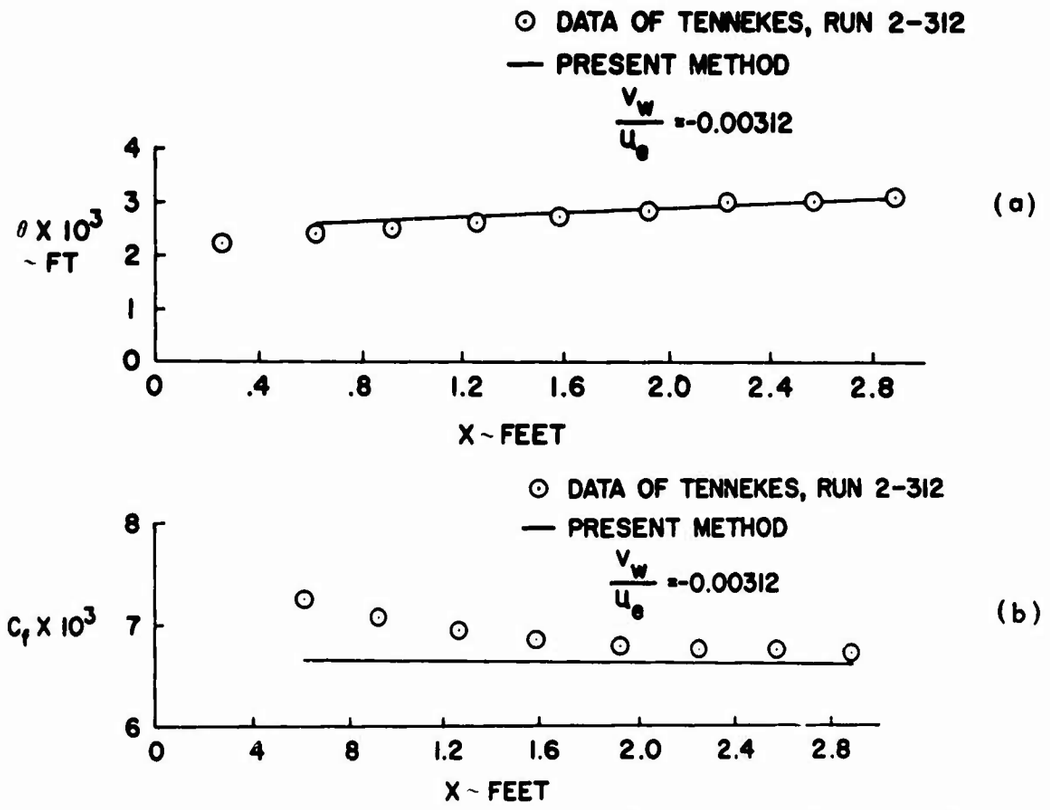

Figure 6. Comparison of calculated and experimental (a) momentum thickness values, and (b) skin-friction values for the sucked boundary layer measured by Tennekes [7].